The Nuclear Factor Erythroid 2–Related Factor 2 Activator Oltipraz Attenuates Chronic Hypoxia–Induced Cardiopulmonary Alterations in Mice

Shunsuke Eba[1], Yasushi Hoshikawa[1], Takashi Moriguchi[2], Yoichiro Mitsuishi[2], Hironori Satoh[2], Kazuyuki Ishida[3], Tatsuaki Watanabe[1], Toru Shimizu[4], Hiroaki Shimokawa[4], Yoshinori Okada[1], Masayuki Yamamoto[2], and Takashi Kondo[1]

[1]Department of Thoracic Surgery, Institute of Development, Aging and Cancer, Tohoku University; [2]Department of Medical Biochemistry, Tohoku University Graduate School of Medicine; [3]Department of Diagnostic Pathology, Iwate Medical University School of Medicine; and [4]Department of Cardiovascular Medicine, Tohoku University Graduate School of Medicine, Sendai, Japan

Nuclear factor erythroid 2–related factor 2 (Nrf2) is a key regulator that activates many antioxidant enzymes. Oxidative stress, which accumulates in diseased lungs associated with pulmonary hypertension (PH), is thought to be responsible for the progression of cardiopulmonary changes. To test whether Nrf2 activation would exert therapeutic efficacy against cardiopulmonary changes in a hypoxia-induced PH model, wild-type (WT) and Nrf2-deficient mice as well as Kelch-like ECH associating protein 1 (Keap1) (negative regulator of Nrf2) knockdown mutant mice were exposed to hypobaric hypoxia for 3 weeks. This chronic hypoxia exacerbated right ventricular systolic pressure, right ventricular hypertrophy (RVH), and pulmonary vascular remodeling in the WT mice. These pathological changes were associated with aberrant accumulation of Tenascin-C, a disease-indicative extracellular glycoprotein. Simultaneous administration of oltipraz, a potent Nrf2 activator, significantly attenuated RVH and pulmonary vascular remodeling and concomitantly ameliorated Tenascin-C accumulation in the hypoxic mice. Hypoxia-exposed Nrf2-deficient mice developed more pronounced RVH than WT mice, whereas hypoxia-exposed Keap1-knockdown mice showed less RVH and pulmonary vascular remodeling than WT mice, underscoring the beneficial potency of Nrf2 activity against PH. We also demonstrated that expression of the Nrf2-regulated antioxidant enzymes was decreased in a patient with chronic obstructive pulmonary disease associated with PH. The decreased antioxidant enzymes may underlie the pathogenesis of cardiopulmonary changes in the patient with chronic obstructive pulmonary disease and PH. The pharmacologically or genetically induced Nrf2 activity clearly decreased RVH and pulmonary vascular remodeling in the hypoxic PH model. The efficacy of oltipraz highlights a promising therapeutic potency of Nrf2 activators for the prevention of PH in patients with hypoxemic lung disease.

Keywords: Nrf2; Keap1; pulmonary vascular remodeling; chronic hypoxia; reactive oxygen species

Chronic hypoxia represents a pathophysiological insult; it induces pulmonary hypertension (PH), which is characterized by right ventricular hypertrophy (RVH) and pulmonary vascular remodeling in humans and animal models at higher altitudes (1–4). These pathophysiological changes to the cardiopulmonary system have been deemed critical exacerbating factors that determine the prognosis of patients suffering from various respiratory diseases presenting with hypoxemia, including chronic obstructive pulmonary disease (COPD) and idiopathic pulmonary fibrosis (IPF) (5, 6). Therefore, intense efforts have been exerted to elucidate the etiological basis of PH in the hopes of finding novel therapeutic targets. Exposure to hypoxic stress has been shown to induce overproduction of reactive oxygen species (ROS) in multiple animal models (7, 8), which leads to the progression of pulmonary vascular remodeling by up-regulating several humoral and intracellular signaling factors that induce vascular remodeling, namely vascular endothelial growth factor, platelet-activating factor, and mitogen-activated protein kinase, in pulmonary arterial endothelial and smooth muscle cells (9–14). Several years ago, we demonstrated that simultaneous treatment with antioxidant N-acetylcysteine dramatically attenuates the pathophysiological changes induced by chronic hypoxic exposure in rats (7). The therapeutic effect of N-acetylcysteine treatment is associated with significant decreases in the phosphatidylcholine hydroperoxide level in the lung tissue (7). These results indicate that the accumulation of ROS induced by chronic exposure to hypoxia probably contributes to the pathogenesis and progression of pulmonary vascular remodeling and the subsequent occurrence of PH.

Nuclear factor erythroid 2–related factor 2 (Nrf2) is a basic region leucine zipper transcription factor that serves as a key regulator of cellular defense against oxidative stress (15). In the absence of oxidative stress stimuli, Nrf2 is rapidly degraded by the ubiquitin-proteasome pathway through association with Kelch-like ECH associating protein 1 (Keap1), a cullin3-based ubiquitin E3 ligase (16, 17). Upon exposure to oxidative stress, Keap1 is inactivated through chemical modification of its cysteine residues. Nrf2 is thereby liberated from Keap1-mediated degradation and subsequently translocates to the nucleus, where it dimerizes with a member of the small Maf family of proteins. This heterodimerized complex activates the transcription of a wide range of antioxidant genes, including NAD phosphate reduced quinone oxidoreductase (NQO1), glutathione S-transferase, glutamate–cysteine ligase catalytic subunit (GCLC), and hemoxygenase-1 (HO-1) via a *cis*-acting DNA element known as antioxidant responsive element. Thus, the molecular basis of the Nrf2-mediated antioxidative stress response is attributed to the increased transcription of antioxidant enzyme genes that accelerate the clearance of ROS-mediated cellular damage (15).

Given the central role of Nrf2 in the antioxidant response, we hypothesized that pharmacological activation of the Nrf2 pathway might exert therapeutic efficacy in a chronic hypoxia–induced murine PH model. The results of this study were consistent with this hypothesis. Chronic administration of the highly potent Nrf2 activator oltipraz significantly decreased pulmonary vascular remodeling and RVH associated with chronic

(*Received in original form December 14, 2011 and in final form January 31, 2013*)

This work was supported by Grant-in-Aid for Scientific Research no. 23,592,052 (Y.H.) from the Japan Society for the Promotion of Science and by a Research Resident Fellowship from Promotion of Cancer Research Japan for the 3rd Term Comprehensive 10-Year Strategy for Cancer Control (H.S.).

Correspondence and requests for reprints should be addressed to Yasushi Hoshikawa, M.D., Department of Thoracic Surgery, Institute of Development, Aging and Cancer, Tohoku University, 4-1 Seiryo-machi, Aoba-ku, Sendai 980-8575 Japan. E-mail: hsohikawa@idac.tohoku.ac.jp

This article has an online supplement, which is accessible from this issue's table of contents at www.atsjournals.org

Am J Respir Cell Mol Biol Vol 49, Iss. 2, pp 324–333, Aug 2013

Originally Published in Press as DOI: 10.1165/rcmb.2011-0396OC on April 3, 2013
Internet address: www.atsjournals.org

hypoxia–induced PH. This favorable therapeutic effect exerted by oltipraz administration was not observed in the Nrf2-deficient ($Nrf2^{-/-}$) mice, indicating that the efficacy of oltipraz was highly dependent on Nrf2 activity. Moreover, we demonstrated that chronic hypoxia–induced pulmonary vascular remodeling and RVH were significantly attenuated in Keap1 knockdown ($Keap1^{f/f}$) mice in which the nuclear Nrf2 protein is constitutively accumulated because of the decreased Keap1 expression (18).

Tenascin-C (TN-C) is a representative extracellular matrix glycoprotein, the expression level of which is known to be associated with the disease progression of PH (19, 20). It has been reported that the bleomycin-induced lung fibrosis model abundantly accumulated TN-C in $Nrf2^{-/-}$ mice compared with $Nrf2^{+/+}$ mice (21), indicating that Nrf2 activity plays an important role in reducing TN-C expression. Indeed, lung TN-C expression was increased in $Nrf2^{+/+}$ mice after 1 week of hypoxic exposure, whereas this hypoxia-induced increase in TN-C expression was significantly reduced by the oltipraz treatment.

In summary, these results strongly suggest that Nrf2 plays a crucial physiological role in the modulation of the cardiopulmonary response to chronic hypoxia. The efficacy of oltipraz highlights the promising therapeutic potency of Nrf2 activators for the prevention of PH associated with severe respiratory diseases presenting with hypoxemia.

MATERIALS AND METHODS

Further details are provided in the online supplement.

Animals and Treatments

$Nrf2^{-/-}$ and $Keap1^{f/f}$ mice backcrossed to a C57BL/6J genetic background were used in this study (18, 22). Mice were matched to wild-type (WT) ($Nrf2^{+/+}$) control mice by weight and age. The mice were exposed to hypoxia using a hypobaric chamber (Shizume Medical, Tokyo, Japan) at a simulated altitude of 17,000 feet as described previously (23). The mice were treated with oltipraz (5, 50, or 500 mg/kg in 0.1 ml of 1% cremophor and 25% glycerol; LKT Laboratories, Inc., St. Paul, MN) by gavage or vehicle every 24 hours. All protocols were approved by the Tohoku University Animal Care Committee (Sendai, Japan).

Immunoblotting Analyses

Nuclear extracts were prepared from the left lungs of the mice using the NE-PER Nuclear and Cytoplasmic Extraction Reagent kit (Thermo Scientific, Waltham, MA). Immunoblotting analysis was performed using anti-Nrf2 and anti-LaminB antibodies (Santa Cruz Biotechnology, Santa Cruz, CA) as reported previously (16).

Real-Time qRT-PCR

Total RNA was extracted from lung tissue using ISOGEN (Nippon Gene, Toyama, Japan). qRT-PCR was performed using an ABI PRISM 7000 sequence detector system (PE-Applied Biosystems, Foster City, CA) and SYBR Premix Ex Taq II (TaKaRa, Shiga, Japan) as described previously (18).The primer sequences for Nrf2, NQO1, GCLC, HO-1, TN-C, β-actin, and 18 s rRNA are shown in Table E1 in the online supplement.

Measurement of Right Ventricular Systolic Pressure and Right Ventricular Hypertrophy

Right ventricular systolic pressure (RVSP) was measured by a direct puncture method as described previously (24). The weight of the right ventricular (RV) free wall and that of the left ventricle and septum (LV + S) were measured separately, and their ratio, RV/(LV + S), was calculated to estimate RVH (24).

Immunohistochemistry

The right lungs of the mice were fixed in an inflated state with 10% buffered formaldehyde solution, and paraffin sections were processed for immunostaining. Mouse anti–α smooth muscle actin (α-SMA) antibody (DAKO, Glostrup, Denmark) and goat anti–Tenascin-C antibody (Santa Cruz Biotechnology) were used. For visualization, tissue sections were incubated with horseradish peroxidase–conjugated antirabbit secondary antibody (Invitrogen, Carlsbad, CA) and detected using the avidin-biotin-peroxidase system (Nichirei Corp., Tokyo, Japan).

Morphometric Analysis of the Pulmonary Arteries

Hilar sections of each right lung were subjected to α-SMA immunohistochemistry analysis and microscopically assessed for remodeling of pulmonary arteries (PAs) as described previously (23, 24).

Flow Cytometry

Single-cell suspensions of lung tissue were prepared as previously described (25) for ROS quantification by flow cytometry using 2′,7′-dichlorodihydrofluoresceindiacetate (DCFDA) (Invitrogen) fluorescence and qRT-PCR of antioxidant genes.

Statistical Analyses

All values are expressed as mean ± SEM. Comparisons were made using one-way ANOVA with Tukey's multiple comparison and unpaired *t* tests. A P value of < 0.05 was considered statistically significant.

RESULTS

Oltipraz Treatment Induces the Nrf2 Regulatory Pathway in Lung Tissue

Immunoblot analysis using whole lung nuclear extracts showed significantly higher nuclear accumulation of Nrf2 protein after oltipraz treatment (50 mg/kg/d for 3 d) in $Nrf2^{+/+}$ mice ($^*P < 0.05$ versus vehicle-treated $Nrf2^{+/+}$ values) (Figures 1A [*left panel*] and 1B). In contrast, Nrf2 accumulation was virtually absent in the lungs of $Nrf2^{-/-}$ mice even with oltipraz (500 mg/kg) treatment (Figure 1A). Vehicle-treated $Keap1^{f/f}$ mice showed the abundant accumulation of Nrf2 protein, reaching a level almost equivalent to that in $Nrf2^{+/+}$ mice treated with 500 mg/kg (Figures 1A [*right panel*] and 1B). Oltipraz treatment (500 mg/kg) rarely induced an additional increase in nuclear Nrf2 protein in $Keap1^{f/f}$ mice (Figures 1A [*right panel*] and 1B).

Despite the accumulated Nrf2 protein, qRT-PCR showed that Nrf2 mRNA expression level in the lung was not substantially changed at 24 hours after a single administration of oltipraz (5, 50, or 500 mg/kg) in $Nrf2^{+/+}$ mice (Figure 1C). As expected, Nrf2 mRNA expression was not detected in the lungs of $Nrf2^{-/-}$ mice regardless of oltipraz treatment (Figure 1C). The mRNA expression of NQO1 and GCLC in the lungs of $Nrf2^{+/+}$ mice was induced by oltipraz treatment in a dose-dependent manner (Figures 1D and 1E). In contrast, inducible expression of these genes was barely detectable in $Nrf2^{-/-}$ mice administered oltipraz at 500 mg/kg. After a single administration of oltipraz (50 mg/kg) to $Nrf2^{+/+}$ mice, the lung NQO1 mRNA expression level began to increase at 12 hours, reached a maximum at 24 hours, and then tended to decline, and it was maintained at high levels compared with the control level at 36 and 48 hours (Figure 1F). The lung GCLC mRNA expression level after a single oltipraz dose (50 mg/kg) followed a similar pattern as NQO1 (Figure 1G). Overall, these observations indicated that oltipraz induced nuclear accumulation of Nrf2 protein in the mouse lung, thereby activating NQO1 and GCLC expression.

Chronic Hypoxia-Induced Cardiopulmonary Changes Are Attenuated by Oltipraz Administration: Pharmacological Activation of Nrf2

To test the therapeutic efficacy of oltipraz on cardiopulmonary pathogenesis associated with chronic hypoxia–induced PH, we

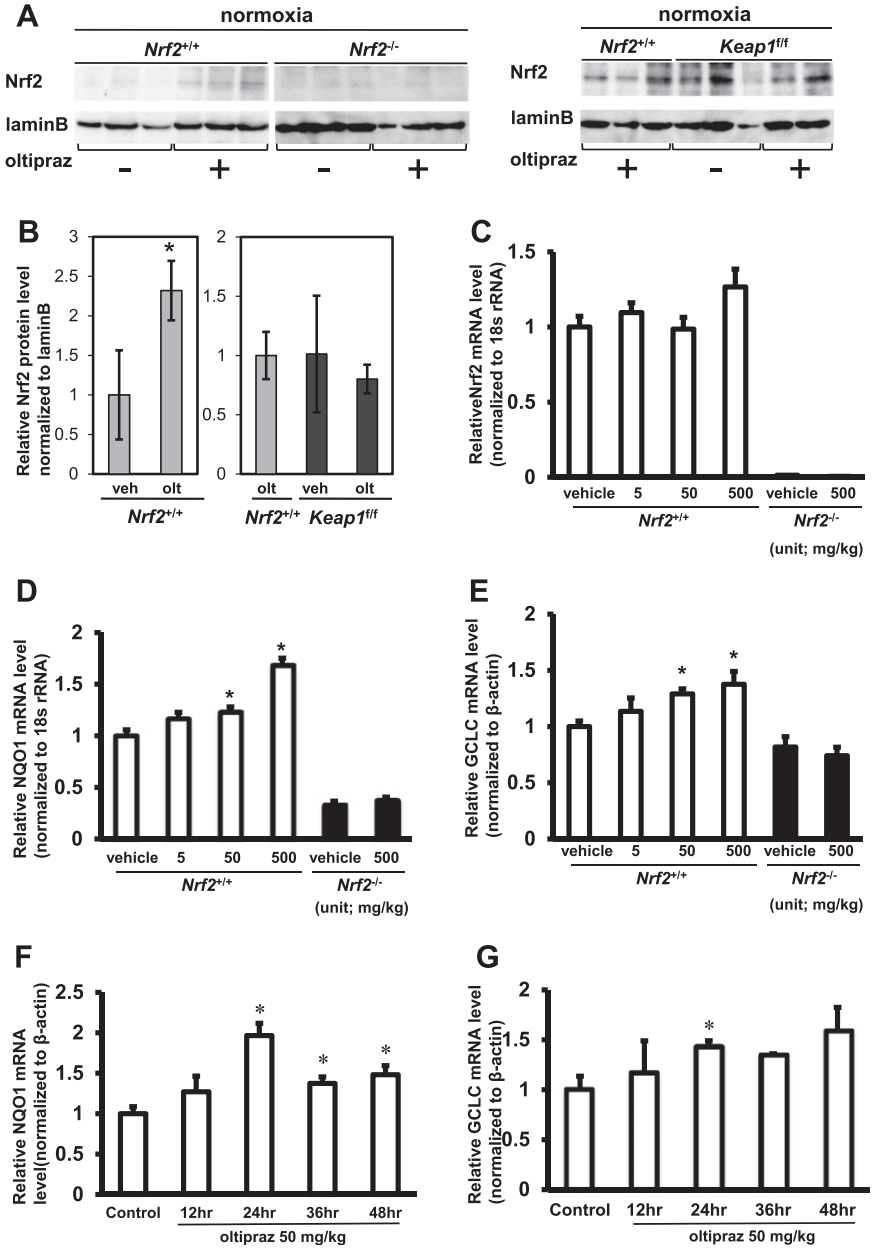

Figure 1. Effects of oltipraz treatment on nuclear Nrf2 (nuclear factor erythroid 2–related factor 2) protein accumulation (*A* and *B*) and Nrf2 mRNA expression (*C*), NAD(P)H quinone oxidoreductase (NQO1) (*D* and *F*), and glutamate–cysteine ligase catalytic subunit (GCLC) (*E* and *G*) in mouse whole lung tissue. (*A*) Effects of oltipraz treatment on nuclear Nrf2 protein accumulation in lung tissues. Nuclear Nrf2 protein accumulation was significantly higher in $Nrf2^{+/+}$ mice treated with oltipraz (50 mg/kg/d for 3 d; $n = 3$) than in vehicle-treated $Nrf2^{+/+}$ mice ($n = 3$) (*$P < 0.05$ compared with $Nrf2^{+/++}$ vehicle values). Nrf2 protein accumulation was not observed in $Nrf2^{-/-}$ mice with or without oltipraz treatment (500 mg/kg). The vehicle-treated $Keap1^{f/f}$ mice showed a high accumulation of Nrf2 protein, reaching a level almost equivalent to that of $Nrf2^{+/+}$ mice treated with 500 mg/kg oltipraz. Oltipraz treatment rarely led to an additional increase in nuclear Nrf2 protein in the $Keap1^{f/f}$ mice. (*B*) Densitometric quantification of the Western blot protein bands of Nrf2 normalized to lamin B. olt = oltipraz; veh = vehicle. (*C*) qRT-PCR showed that $Nrf2^{+/+}$ mice treated with vehicle and oltipraz (5, 50, and 500 mg/kg) ($n = 4$ each) did not differ in Nrf2 mRNA expression levels. Nrf2 mRNA expression was not detected in the lungs of the $Nrf2^{-/-}$ mice regardless of oltipraz treatment (500 mg/kg) ($n = 5$ each). (*D* and *E*) The mRNA expression of NQO1 (*D*) (vehicle, $n = 5$; oltipraz 5 mg/kg, $n = 3$; 50 mg/kg, $n = 5$; 500 mg/kg, $n = 4$) and GCLC (*E*) ($n = 4$ each) mRNA in the lungs of $Nrf2^{+/+}$ mice was induced by oltipraz in a dose-dependent manner (NQO1: vehicle, 1.00 ± 0.06; oltipraz 5 mg/kg, 1.16 ± 0.07; 50 mg/kg, 1.23 ± 0.05*; 500 mg/kg, 1.67 ± 0.08*; GCLC: vehicle, 1.00 ± 0.05; oltipraz 5 mg/kg, 1.13 ± 0.12; 50 mg/kg, 1.29 ± 0.05*; 500 mg/kg, 1.38 ± 0.11*; *$P < 0.05$ versus vehicle values). Inducible expression of NQO1 (*D*) and GCLC (*E*) mRNA was barely detectable in $Nrf2^{-/-}$ mice administered oltipraz (500 mg/kg) ($n = 5$ each). (*F* and *G*) After a single oltipraz dose (50 mg/kg) to $Nrf2^{+/+}$ mice, the lung NQO1 mRNA expression level began to increase at 12 hours (1.27 ± 0.19 versus 1.00 ± 0.09 for the control), reached a maximum at 24 hours (1.97 ± 0.15*), and then declined; however, it was maintained at higher levels at 36 (1.37 ± 0.08*) and 48 hours (1.48 ± 0.11*) (*$P < 0.05$ versus control values) compared with control levels ($n = 3$ each) (*F*). The lung GCLC mRNA expression level after a single treatment of 50 mg/kg oltipraz followed a similar pattern to NQO1 (control, 1.00 ± 0.14; 12 h, 1.17 ± 0.32; 24 h, 1.43 ± 0.06*; 36 h, 1.35 ± 0.01; 48 h, 1.58 ± 0.24 [$n = 3$ each]) (*$P < 0.05$ versus control values) (*G*).

exposed $Nrf2^{+/+}$ mice to hypobaric hypoxia for 3 weeks and simultaneously administered vehicle or 50 mg/kg of oltipraz 5 days a week for 3 weeks. The doses and frequency of oltipraz administration were determined on the basis of the efficient inducibility of NQO1 and GCLC mRNA expression at 24 hours after administration of oltipraz (50 mg/kg) (Figures 1D–1G). Changing the dose and frequency of oltipraz to 500 mg/kg once a week resulted in almost similar inhibitory effects in the following experiments (data not shown) (26). Mice subjected to the hypoxic exposure showed barely any gains in body weight, whereas age-matched control mice exposed to normoxic conditions showed normal weight gain regardless of oltipraz administration (*see* Figure E1 in the online supplement). Hematocrit levels were increased up to 60% in the hypoxic mice, whereas those of normoxic mice were around 40% on average (Table E2). Oltipraz administration had no effect on hematocrit levels in normoxia or hypoxia (Table E2).

Three weeks of hypoxic exposure led to the development of PH (i.e., an increase in RVSP values) and RVH (i.e., an increase in the RV/[LV + S] ratio) in vehicle-treated $Nrf2^{+/+}$ mice (Table 1). Oltipraz administration significantly decreased hypoxia-induced RVH, whereas this medication exerted no effect on the increased RVSP in hypoxic $Nrf2^{+/+}$ mice, indicating that pharmacological activation of Nrf2 had a pronounced effect in reducing hypoxia-associated RVH without reducing RVSP (Table 1). Under normoxic conditions, oltipraz had no effect on RVSP or the RV/(LV + S) ratio in $Nrf2^{+/+}$ mice (Table 1).

To evaluate muscularization of the small pulmonary arterioles around the level of the alveolar duct, the number of nonmuscular, partially muscular, and fully muscular vessels was counted in lung sections from each mouse by means of immunohistochemistry for

TABLE 1. EFFECTS OF OLTIPRAZ ON HYPOXIA-INDUCED PULMONARY HYPERTENSION, RIGHT VENTRICULAR HYPERTROPHY, MUSCULARIZATION OF SMALL PULMONARY ARTERIOLES, AND VESSEL WALL THICKNESS OF THE PULMONARY ARTERIES OF *Nrf2*$^{+/+}$ (WILD-TYPE) MICE AFTER 3 WEEKS OF EXPOSURE TO HYPOXIA

	Normoxia		Hypoxia	
Measurements	Vehicle	Oltipraz	Vehicle	Oltipraz
RVSP, mm Hg	26.8 ± 1.4 (10)*	24.0 ± 1.1 (7)	30.2 ± 0.9† (8)	31.5 ± 1.0† (10)
RV/(LV + S)	0.27 ± 0.02 (10)	0.25 ± 0.01 (10)	0.41 ± 0.02† (10)	0.36 ± 0.01†‡ (10)
Muscularization of small PA ($n = 5$), %				
Nonmuscular	80.8 ± 1.3	83.0 ± 2.3	51.4 ± 1.7†	62.4 ± 2.2†‡
Partially muscular	17.0 ± 1.3	15.4 ± 2.5	39.4 ± 1.3†	32.8 ± 2.1†‡
Fully muscular	2.2 ± 0.6	1.6 ± 0.5	9.2 ± 0.4†	4.8 ± 0.4†‡
VWT of PAs	0.180 ± 0.004 (5)	0.178 ± 0.004 (5)	0.252 ± 0.004† (5)	0.199 ± 0.004†‡ (5)

Definition of abbreviations: PAs = pulmonary arteries; RV/(LV + S) = ratio of the right ventricular free wall to the combined weight of the left ventricle + septum; RVSP = right ventricular systolic pressure; VWT = vessel wall thickness ([external diameter of PA − internal diameter]/external diameter).

*Values are mean ± SE. Number of mice is indicated in parentheses.

† $P < 0.05$ versus normoxia + vehicle.

‡ $P < 0.05$ versus hypoxia + vehicle.

α-SMA (*see* the online supplement for categorization). More than 80% of pulmonary arterioles in the vehicle-treated normoxic *Nrf2*$^{+/+}$ mice exhibited nonmuscular vessels, whereas the remaining 19% of arterioles had partially (17.0%) or fully (2.2%) muscular walls. In contrast, in hypoxic *Nrf2*$^{+/+}$ mice, the number of partially or fully muscular pulmonary arterioles was significantly increased to 39.4 and 9.2%, respectively. The proportion of nonmuscular pulmonary arterioles was decreased to 51.4% (Table 1). Oltipraz administration significantly decreased the muscularization of the pulmonary arterioles in hypoxic *Nrf2*$^{+/+}$ mice. The proportion of nonmuscular vessels recovered to 62.4%, and that of partially and fully muscular pulmonary arterioles decreased to 32.8 and 4.8%, respectively, in oltipraz-treated hypoxic *Nrf2*$^{+/+}$ mice. In addition, chronically hypoxic *Nrf2*$^{+/+}$ mice showed increased vessel wall thickness (VWT) of the PAs at the level of the terminal bronchiole (TB) when compared with normoxic *Nrf2*$^{+/+}$ mice (Table 1). As expected, VWT of the oltipraz-treated hypoxic mice was significantly lower than that of the vehicle-treated hypoxic mice (Table 1). In summary, oltipraz administration significantly attenuated the pathogenic muscularization of PA, which presumably contributed to the improvement in RVH under chronic hypoxia. In contrast, oltipraz treatment had no effect on elevated RVSP.

Nrf2-Deficient Mice Developed More Severe RVH with a Similar Degree of Pulmonary Vascular Remodeling

To address the physiological significance of Nrf2 under hypoxia, we subjected *Nrf2*$^{-/-}$ mice to 3 weeks of hypoxic exposure. *Nrf2*$^{-/-}$ mice exhibited a significantly higher RV/(LV + S) ratio than WT mice, whereas the muscularization of their small pulmonary arterioles and VWT of their PAs were not significantly changed compared with hypoxic WT mice (Table 2). In contrast, *Nrf2*$^{-/-}$ mice showed significantly less RVSP than WT mice after hypoxic exposure (Table 2) (*see* DISCUSSION). Oltipraz- and vehicle-treated *Nrf2*$^{-/-}$ mice did not differ in terms of RVH (Figure 2A), muscularization of their small pulmonary arterioles (Figure 2B), and VWT of their PA (Figure 2C) after 3-weeks of exposure to hypobaric hypoxia. These results indicate that Nrf2 plays a crucial role in the prevention of chronic hypoxia–induced RVH and that the therapeutic efficacy of oltipraz against the hypoxia-induced cardiopulmonary changes was completely lost in *Nrf2*$^{-/-}$ mice.

Chronic Hypoxia-Induced RVH and Pulmonary Vascular Remodeling Are Attenuated in *Keap1*$^{f/f}$ Mice: Genetic Activation of Nrf2

To investigate the consequences of forced Nrf2 activation, we used *Keap1*$^{f/f}$ mice (18). After the 3-week exposure to

TABLE 2. EFFECTS OF Nrf2 KNOCKOUT ON HYPOXIA-INDUCED PULMONARY HYPERTENSION, RIGHT VENTRICULAR HYPERTROPHY, MUSCULARIZATION OF SMALL PULMONARY ARTERIOLES, AND VESSEL WALL THICKNESS OF THE PULMONARY ARTERIES AFTER 3 WEEKS OF EXPOSURE TO HYPOXIA

	Normoxia		Hypoxia	
Measurements	*Nrf2*$^{+/+}$	*Nrf2*$^{-/-}$	*Nrf2*$^{+/+}$	*Nrf2*$^{-/-}$
RVSP, mm Hg	24.4 ± 0.7 (13)*	22.2 ± 0.9 (11)	34.8 ± 1.1† (17)	29.2 ± 1.0‡§ (12)
RV/(LV + S)	0.23 ± 0.01 (9)	0.28 ± 0.02 (4)	0.40 ± 0.01† (17)	0.467 ± 0.01‡§ (12)
Muscularization of small PA	(4)	(4)	(7)	()
Nonmuscular, %	81.8 ± 0.6	78.8 ± 0.5	54.7 ± 1.4†	50.9 ± 2.6‡
Partially muscular, %	17.0 ± 0.7	19.0 ± 0.4	37.6 ± 0.9†	43.9 ± 2.7‡
Fully muscular, %	1.3 ± 0.3	2.3 ± 0.5	7.7 ± 2.5†	5.3 ± 0.8†
VWT of PAs	0.214 ± 0.005 (4)	0.209 ± 0.006 (4)	0.262 ± 0.005† (4)	0.248 ± 0.006‡ (4)

Definition of abbreviations: *Nrf2*$^{+/+}$ = wild-type mice; *Nrf2*$^{-/-}$ = Nrf2 knockdown mice; PAs = pulmonary arteries; RV/(LV + S) = ratio of the right ventricular free wall to the combined weight of the left ventricle + septum; RVSP = right ventricular systolic pressure; VWT = vessel wall thickness ([external diameter of PA − internal diameter]/external diameter).

*Values are mean ± SE. Number of mice is indicated in parentheses.

† $P < 0.05$ versus *Nrf2*$^{+/+}$ + normoxia.

‡ $P < 0.05$ versus *Nrf2*$^{-/-}$ + normoxia.

§ $P < 0.05$ versus *Nrf2*$^{+/+}$ + hypoxia.

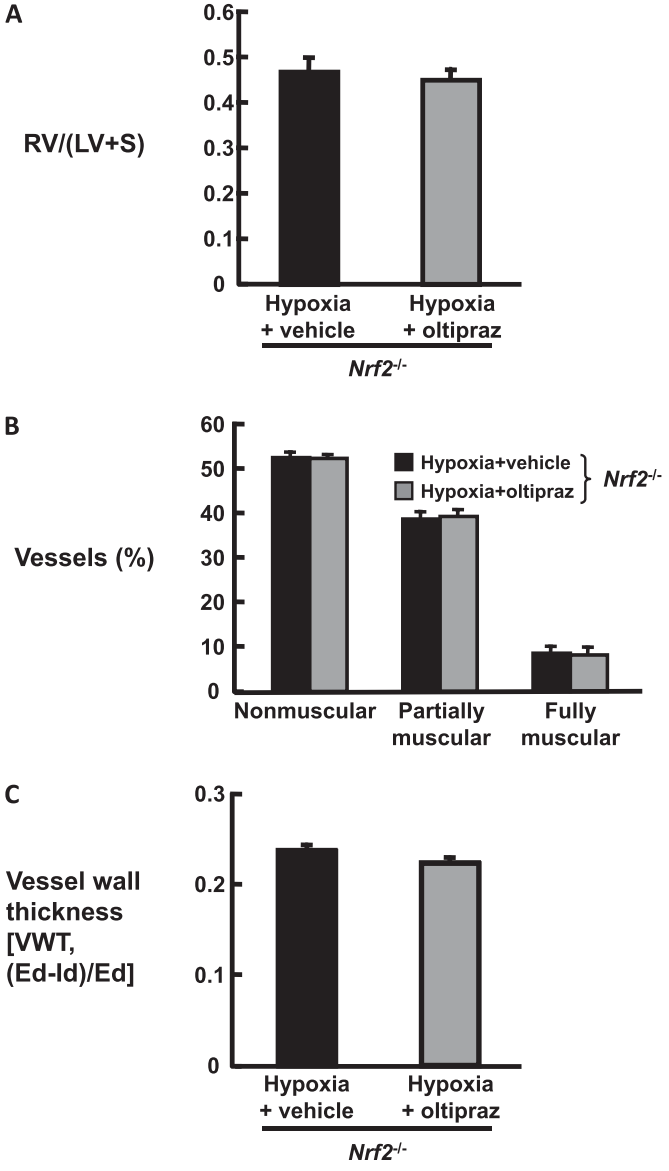

Figure 2. Effects of oltipraz treatment on hypoxia-induced right ventricular hypertrophy (RVH) (*A*), muscularization of small pulmonary arterioles corresponding to the level of the alveolar duct (< 25 μm) (*B*), and vessel wall thickness (VWT) of the pulmonary arteries corresponding to the level of the terminal bronchiole (30–50 μm) (*C*) in *Nrf2*$^{-/-}$ mice. (*A*) Oltipraz-treated ($n = 8$) and vehicle-treated ($n = 7$) *Nrf2*$^{-/-}$ mice did not differ in terms of RVH, as indicated by the ratio of the right ventricular free wall to the combined weight of the left ventricle + septum [RV/(LV + S)] after 3 weeks of exposure to hypobaric hypoxia (0.47 ± 0.03 versus 0.45 ± 0.02; not significant). (*B*) Muscularization of the small pulmonary arterioles was evaluated by counting the number of nonmuscular, partially muscular, and fully muscular vessels in the lung sections of mice used for immunohistochemistry analysis of α smooth muscle actin. The distribution of nonmuscular, partially muscular, and fully muscularized small arterioles did not differ between hypoxia-exposed *Nrf2*$^{-/-}$ mice treated with oltipraz ($n = 5$) and mice treated with vehicle ($n = 5$) (nonmuscular, 52.6 ± 1.1% versus 52.4 ± 0.7%, ns; partially muscular, 38.8 ± 1.5% versus 39.4 ± 1.3%, ns; fully muscular, 8.6 ± 1.4% versus 8.2 ± 1.5%; not significant). (*C*) VWT was calculated as the external diameter (Ed) minus the internal diameter (Id) divided by the external diameter: (Ed − Id)/Ed. VWT of *Nrf2*$^{-/-}$ mice treated with the oltipraz ($n = 5$) and vehicle-treated mice ($n = 5$) (0.237 ± 0.006 versus 0.224 ± 0.005; ns) was similar after chronic hypoxic exposure.

hypobaric hypoxia, *Keap1*$^{f/f}$ mice developed significantly less RVH than WT mice (Table 3). PA muscularization and VWT were also attenuated in chronically hypoxic *Keap1*$^{f/f}$ mice compared with hypoxic WT mice, indicating the similar efficacy of genetic activation of Nrf2 toward cardiopulmonary alterations (Table 3). However, *Keap1*$^{f/f}$ mice exhibited a sustained increase in RVSP after exposure to chronic hypoxia (Table 3). This observation was in good agreement with the diminished efficacy of oltipraz treatment against elevated RV pressure in hypoxic WT mice.

Increased ROS Accumulation in CD31$^+$ Pulmonary Vascular Endothelial Cells upon Hypoxic Exposure

We next tried to quantitatively assess ROS accumulation using DCFDA (a fluorescent ROS indicator) in CD31$^+$ pulmonary vascular endothelial cells (PVECs). Expectedly, the DCFDA level in lung CD31$^+$ cells from *Nrf2*$^{+/+}$ mice after 2 days of hypoxia exposure was significantly higher than that from normoxic *Nrf2*$^{+/+}$ mice (Figures 3A and 3B). Furthermore, hypoxia-exposed *Nrf2*$^{-/-}$ mice showed higher ROS accumulation in lung CD31$^+$ cells than hypoxia-exposed *Nrf2*$^{+/+}$ mice. Lung CD31$^+$ cells in *Nrf2*$^{-/-}$ mice displayed a slightly higher DCFDA levels than those in *Nrf2*$^{+/+}$ mice even under normoxia, suggesting a potential role of Nrf2 for ROS clearance in normoxic pulmonary endothelial cells (Figures 3A and 3B).

Antioxidant Genes Are Differentially Expressed in CD31$^+$ PVECs after Hypoxic Exposure

Given the robustly increased ROS accumulation in CD31$^+$ PVECs observed on hypoxic exposure, we examined the inducible expression of Nrf2 target genes. First, we evaluated overall changes in the expression of NQO1 and GCLC in lungs of hypoxia-exposed WT mice by qRT-PCR and immunohistochemistry. Despite increased ROS in the PVECs, NQO1 and GCLC mRNA were decreased in hypoxic WT mice when compared with normoxic WT mice (Figures E3A and E3B). Immunohistochemical analysis revealed that NQO1 was mainly expressed in the PA media (Figures E3C and E3D, *arrows*), whereas GCLC expression was preferentially observed in the endothelium (Figures E3G and E3H, *arrows*). After exposure to hypoxia for 2 days, the NQO1 (Figures E3E and E3F) and GCLC (Figures E3I and E3J) signals became barely detectable in the PA.

To further explore antioxidant gene expression at the cellular level, we examined mRNA expression of Nrf2 and its target genes in the CD31$^+$ endothelial fraction sorted from the lungs of WT mice upon 2 days of hypoxia exposure. Nrf2 mRNA expression levels were not significantly different between the hypoxic and normoxic conditions (Figure 3C). Changes in the NQO1 mRNA levels in the CD31$^+$ cells did not reach statistically significance after 2 days of hypoxia exposure (Figure 3D). In contrast, mRNA expression of GCLC and HO-1 was decreased in the lung CD31$^+$ cells of WT mice after 2 days of hypoxia exposure (Figures 3E and 3F). WT and *Nrf2*$^{-/-}$ mice commonly exhibited low levels of GCLC and HO-1 mRNA expression in lung CD31$^+$ cells under hypoxia (Figures 3E and 3F).

Hypoxia-Induced Pulmonary TN-C Expression Is Attenuated by Oltipraz treatment

To explore the pathological mechanism by which oltipraz decreases the hypoxia-induced pulmonary vascular remodeling in mice, we examined the effect of oltipraz treatment on expression of TN-C, which is an extracellular matrix protein associated

TABLE 3. EFFECTS OF KELCH-LIKE ECH ASSOCIATING PROTEIN 1 KNOCKDOWN ON HYPOXIA-INDUCED PULMONARY HYPERTENSION, RIGHT VENTRICULAR HYPERTROPHY, MUSCULARIZATION OF SMALL PULMONARY ARTERIOLES, AND VESSEL WALL THICKNESS OF THE PULMONARY ARTERIES AFTER 3 WEEKS OF EXPOSURE TO HYPOXIA

	Normoxia		Hypoxia	
Measurements	Wild-type	*Keap1*$^{f/f}$	Wild-type	*Keap1*$^{f/f}$
RVSP	20.8 ± 1.2 (4)*	23.4 ± 0.4 (4)	33.3 ± 0.9† (10)	31.2 ± 1.3‡ (8)
RV/(LV + S)	0.22 ± 0.01 (4)	0.27 ± 0.01 (4)	0.43 ± 0.01† (10)	0.34 ± 0.01‡§ (8)
Muscularization of small PA	(4)	(4)	(4)	(4)
Nonmuscular, %	80.0 ± 1.6	80.0 ± 1.2	46.5 ± 1.0†	59.5 ± 0.9‡§
Partially muscular, %	19.8 ± 1.7	17.8 ± 1.7	47.3 ± 0.9†	36.5 ± 1.0‡§
Fully muscular, %	0.5 ± 0.3	2.0 ± 0.7	6.3 ± 1.4†	4.0 ± 0.7
VWT of PAs	0.186 ± 0.006 (4)	0.201 ± 0.006 (4)	0.245 ± 0.007† (4)	0.219 ± 0.006‡ (4)

Definition of abbreviations: Keap1 = Kelch-like ECH associating protein 1; *Keap1*$^{f/f}$ = Keap1 knockdown mice; PAs = pulmonary arteries; RV/(LV + S) = ratio of the right ventricular free wall to the combined weight of the left ventricle + septum; RVSP = right ventricular systolic pressure; VWT = vessel wall thickness ([external diameter of PA − internal diameter]/external diameter).

*Values are mean ± SE. Number of mice is indicated in parentheses.

$^{\dagger}P < 0.05$ versus wild type + normoxia.

$^{\ddagger}P < 0.05$ vs. *Keap1*$^{f/f}$ + normoxia.

$^{\S}P < 0.05$ versus wild type + hypoxia.

with progression of PH (19, 20). TN-C mRNA abundance in WT mice was significantly increased after 7 days of exposure to hypoxia, as we previously reported (20). Oltipraz treatment attenuated the increased TN-C mRNA levels in hypoxic WT mice (Figure 4A). Concomitantly, immunohistochemical analyses with anti–TN-C antibody demonstrated an increased intensity of TN-C signals in the external elastic lamina of the PA walls in hypoxic WT mice (Figure 4C, *arrows*) compared with normoxic WT mice (Figure 4B). In contrast, the oltipraz administration decreased the TN-C immunoreactivity in the PA walls (Figure 4D, *arrowheads*). Closer examination of lung sections from vehicle-treated hypoxic WT mice revealed that the induced TN-C immunoreactivity was predominantly localized to the PA walls, as shown by the level of the TB (Figures 4E–4G, *arrows*) rather than the level of alveolar duct (Figures 4G and 4H, *arrowheads*). This observation was consistent with the increased VWT of PA in the hypoxic mice, which was detected predominantly around the level of TB (Table 1). Therefore, the oltipraz-mediated improvement in PA wall thickening could be attributed to the decreased TN-C expression in the PA walls around the level of TB.

Diminished Expression of GCLC and NQO1 in a Patient with COPD with PH

We immunohistochemically examined GCLC and NQO1 expression in the pulmonary vasculatures of a patient with COPD suffering from hypoxemia complicated with PH (COPD+PH). GCLC and NQO1 were expressed in the PA endothelial layers of the control lungs (Figures E5A–E5C and E5J–E5L, *arrows*). COPD+PH lung tissues exhibited significantly diminished GCLC and NQO1 expression in the PA walls when compared with controls (Figures E5D–E5F and E5M–E5O). This finding was consistent with the decreased GCLC expression observed in $CD31^{+}$ PVECs from hypoxia-exposed WT mice. In contrast to the lung from the patient with COPD and PH, lungs dissected from the patient with idiopathic pulmonary arterial hypertension (IPAH), in which hypoxemia does not usually occur, showed strong GCLC and NQO1 signals in plexiform lesions and endothelial layers of thickened PA (Figures E5G–E5I and E5P–E5R), presumably in response to ROS accumulation (27).

DISCUSSION

The principal findings of this study are as follows: *1*) Gavage administration of oltipraz, a potent Nrf2 activator, enhanced the expression level of representative antioxidant genes NQO1 and GCLC by inducing nuclear accumulation of Nrf2 protein in mouse lung tissues; *2*) treatment with oltipraz significantly attenuated RVH and pulmonary vascular remodeling associated with the accumulation of TN-C developed after 3-week exposure to hypobaric hypoxia in WT mice; *3*) the favorable therapeutic effect of oltipraz on hypoxia-induced cardiopulmonary changes was not observed in *Nrf2*$^{-/-}$ mice; and *4*) *Keap1*$^{f/f}$ mice showed increased nuclear Nrf2 protein and developed significantly less RVH and pulmonary vascular remodeling after chronic exposure to hypobaric hypoxia compared with WT mice. Collectively, our data strongly indicated that Nrf2 played an important role in the improvement in cardiopulmonary alterations in a hypoxic PH model and that Nrf2 activators may prove to be useful therapies for the PH that often accompanies hypoxemic lung diseases like IPF and COPD.

The Nrf2 activator oltipraz is a substituted dithiolthione that is structurally related to similar chemical groups found in cruciferous vegetables (28). Consumption of these vegetables has been associated with a decreased human cancer risk (28). Indeed, oltipraz has been reported as having chemopreventive activity in a broad spectrum of animal models of carcinogenesis (29–31). The chemopreventive efficacy of oltipraz against gastric neoplasia in benzo[a]pyrene-treated mice was completely inhibited in Nrf2$^{-/-}$ mice (32). Thereafter, the efficacy of oltiprazis was mediated by antioxidant and detoxifying gene expression through Nrf2 activation (32). Modification of critical cysteine residues of Keap1 provides a fundamental mechanism for Nrf2 activation (16, 17). On oxidation of Keap1 cysteine residues, conformational changes led to nuclear Nrf2 accumulation, thereby inducing antioxidant responsive element–mediated transcriptional activation (16, 17). Although a direct reaction of oltipraz with cysteine residues in Keap1 has remained elusive, oltipraz is known to be reactive with thiol groups (33). Through examination of the responsiveness of Keap1 cysteine substitution mutants to oltipraz treatment, we should be able to elucidate the detailed mechanism of oltipraz activity. Oltipraz induces nuclear Nrf2 protein accumulation and expression of Nrf2 target genes in mouse liver (34) and adipose tissue (35). However, whether oltipraz induces Nrf2 activation in the lung remains uncertain. We demonstrated that gavage administration of oltipraz increased Nrf2 nuclear accumulation in lung tissues of WT mice, although the Nrf2 mRNA expression level was not substantially changed. Meanwhile, NQO1 and GCLC expression was clearly induced by oltipraz

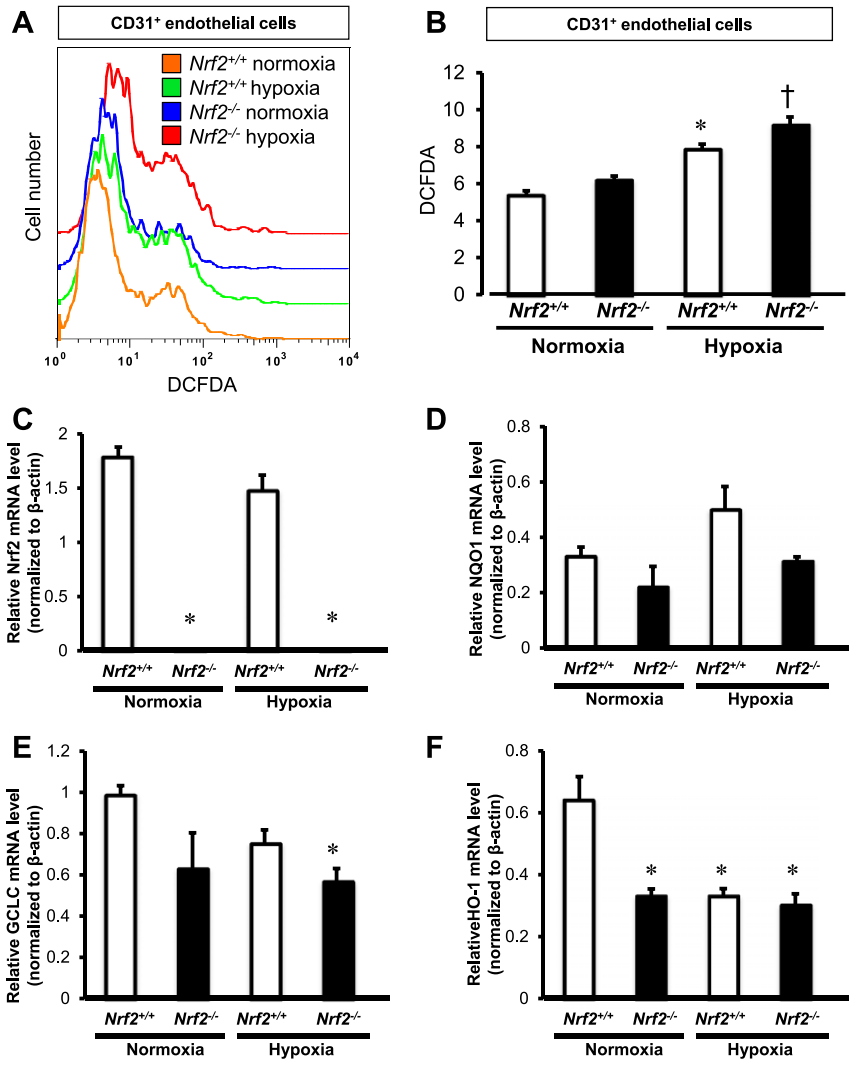

Figure 3. Effects of hypobaric hypoxia on reactive oxygen species (ROS) accumulation (*A* and *B*) and on the Nrf2 mRNA expression level (*C*), NAD(P)H: quinone oxidoreductase (NQO1) (*D*), the glutamate–cysteine ligase catalytic subunit (GCLC) (*E*), and hemoxygenase-1 (HO-1) (*F*) in $CD31^+$ pulmonary vascular endothelial cells (PVECs) from $Nrf2^{+/+}$ and $Nrf2^{-/-}$ mice ($n = 3$ each). (*A*) Representative histogram of the analysis of the ROS level in $CD31^+$ PVECs from $Nrf2^{+/+}$ and $Nrf2^{-/-}$ mice exposed to hypoxic or normoxic conditions for 2 days; assessments were made using 2′,7′-dichlorodihydrofluoresceindiacetate (DCFDA). (*B*) The DCFDA level in lung $CD31^+$ cells from $Nrf2^{+/+}$ mice after 2 days of exposure to hypoxia was significantly higher than that in $Nrf2^{+/+}$ mice exposed to normoxic conditions (7.83 ± 0.30 versus 5.37 ± 0.24; $^*P < 0.05$). Hypoxia-exposed $Nrf2^{-/-}$ mice showed even higher ROS accumulation in lung $CD31^+$ cells than normoxic $Nrf2^{-/-}$ mice (9.14 ± 0.47 versus 6.18 ± 0.23; $^\dagger P < 0.05$). (*C*) $CD31^+$ cells from the lungs of $Nrf2^{+/+}$ mice after 2 days of exposure to hypoxic and normoxic conditions did not differ in terms of Nrf2 mRNA expression levels. Nrf2 mRNA expression was not detected in the lung $CD31^+$ cells of $Nrf2^{-/-}$ mice regardless of hypoxic exposure. (*D*) NQO1 mRNA expression in lung $CD31^+$ cells from $Nrf2^{+/+}$ mice was not significantly altered after 2 days of exposure to hypoxia. $Nrf2^{-/-}$ mice tended to show lower NQO1 mRNA expression in lung $CD31^+$ cells than $Nrf2^{+/+}$ mice under hypoxic and normoxic conditions. (*E*) The expression level of GCLC mRNA tended to decrease in the lung $CD31^+$ cells of $Nrf2^{+/+}$ mice after 2 days of exposure to hypoxia (the difference reached statistical significance when assessed with an unpaired *t* test). $Nrf2^{+/+}$ and $Nrf2^{-/-}$ mice expressed comparable levels of GCLC mRNA in lung $CD31^+$ cells under hypoxia. (*F*) The expression level of HO-1 mRNA was significantly decreased after 2 days of exposure to hypoxia ($^*P < 0.05$). $Nrf2^{+/+}$ and $Nrf2^{-/-}$ mice did not differ in terms of the HO-1 mRNA levels in their lung $CD31^+$ cells under hypoxia.

treatment in a dose-dependent manner. The inducible expression of these genes was barely detectable in $Nrf2^{-/-}$ mice administered oltipraz, indicating that oltipraz activates the expression of the antioxidant genes by inducing nuclear accumulation of Nrf2 protein in the mouse lung.

Chronic oltipraz administration attenuated hypoxia-induced cardiopulmonary alterations, as evidenced by the decreased RV/(LV + S) ratio, improved muscularization of small pulmonary arterioles, and suppressed PA wall thickening. Despite the remarkable improvement in the RVH and pulmonary vascular remodeling after oltipraz treatment in WT mice, the therapeutic efficacy of oltipraz was completely lost in $Nrf2^{-/-}$ mice. Therefore, the pharmacological activity of oltipraz against chronic hypoxia–induced cardiopulmonary alterations critically depends on Nrf2 function.

The preventive function of Nrf2 against chronic hypoxia–induced pulmonary vascular remodeling was further confirmed in the $Keap1^{f/f}$ mice subjected to the same 3-week hypoxic exposure. These mice exhibited marked resistance to chronic hypoxia–induced pulmonary vascular remodeling and RVH, thus indicating an essential Nrf2 function for the prevention of cardiopulmonary alterations in a chronic hypoxia–induced PH model. RVH was substantially exaggerated in $Nrf2^{-/-}$ mice compared with WT control mice. The dilation and hypertrophy of RV in hypoxia-exposed $Nrf2^{-/-}$ mice was macroscopically evident. However, hypoxia-exposed $Nrf2^{-/-}$ mice showed significantly less of an increased RVSP than hypoxic WT mice. Further experiments are required to determine whether this is related to a direct effect of Nrf2 on RV structure and function or whether this simply reflects a failing RV in which the RV can no longer generate an elevated RVSP in the face of the severe vascular remodeling. Other explanations are plausible, and this remains a fertile and important area for future investigation.

A correlation between RVSP and the development of RVH, as assessed by RV/(LV + S), has been reported in a hypoxic PH mouse model (23). However, both types of Nrf2 activation (i.e., oltipraz administration and Keap1 knockdown) hardly exerted any positive effects on improvement of the increased RVSP level, whereas both showed an inhibitory effect against hypoxia-induced RVH and pulmonary vascular remodeling. A plausible explanation for this might be deduced from the function of Rho-kinase signaling in the development of pulmonary vasoconstriction. Hypoxic PH is characterized by not only pulmonary vascular remodeling but also by hypoxic pulmonary vasoconstriction (HPV) (2, 36). Crossno and colleagues reported that rosiglitazone (ROSI), a synthetic peroxisome proliferator-activated receptor (PPAR)-γ ligand, attenuated hypoxia-induced pulmonary vascular remodeling and RVH

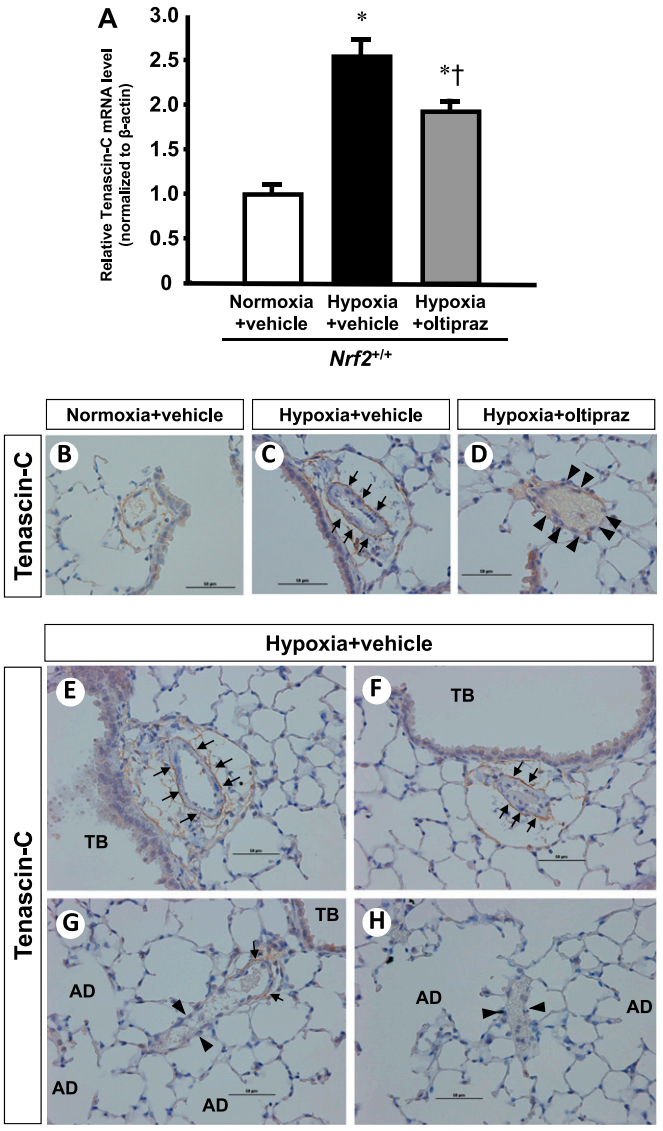

Figure 4. Effects of oltipraz treatment on the hypoxia-induced increase in tenascin-C (TN-C) expression in the lungs of $Nrf2^{+/+}$ mice. (*A*) qRT-PCR revealed that TN-C mRNA expression in the lungs of $Nrf2^{+/+}$ mice was significantly increased by 7 days of hypoxia exposure ($n = 4$ each; normoxia + vehicle, 1.00 ± 0.11 versus hypoxia + vehicle, 2.55 ± 0.18; $^{*}P < 0.05$). Oltipraz treatment (50 mg/kg/d for the entire 7 d of hypoxic exposure) significantly attenuated the increase in lung TN-C mRNA levels caused by hypoxia ($n = 4$ each; hypoxia + oltipraz, 1.93 ± 0.11; $^{\dagger}P < 0.05$ versus hypoxia + vehicle levels). (*B–H*) Representative TN-C expression pattern (*brown staining*) detected by immunohistochemistry (original magnification: ×400; *bar* represents 50 μm). AD = alveolar duct; TB = terminal bronchiole. (*B*) Normoxic lung of a $Nrf2^{+/+}$ mouse demonstrating faint staining for TN-C in bronchial epithelial cells and in the external elastic lamina of the pulmonary artery wall. (*C*) $Nrf2^{+/+}$ mice exposed to hypoxia for 7 days without oltipraz treatment showed strong TN-C expression in the external elastic lamina of the pulmonary artery wall. (*D*) Hypoxic $Nrf2^{+/+}$ mice simultaneously treated with oltipraz showed decreased immunoreactivity to TN-C in the pulmonary artery wall compared with the vehicle-treated hypoxic mice (*C*). (*E–H*) Close examination of lung sections from vehicle-treated hypoxic $Nrf2^{+/+}$ mice revealed brown signals for TN-C in the pulmonary artery walls corresponding to the level of the terminal bronchiole (TB) (*E*, *F*, and *arrows* in *G*); no stains were seen at the level of the alveolar duct (AD) (*G* and *H*, *arrowheads*).

but failed to decrease the development of hypoxic PH in rats (37). Because Rho-kinase signaling emerged as a major contributor to HPV pathogenesis, they administered a Rho-kinase inhibitor to hypoxic PH rats and successfully reduced the high PA pressure to almost normal levels. Given this, Crossno and colleagues concluded that ROSI failed to block hypoxia-induced PH primarily because of its inability to repress the sustained Rho-kinase–mediated HPV. PPARγ and Nrf2 functionally interact to synergistically elicit the protection against oxidative lung injury (38). PPARγ expression level is up-regulated by Nrf2, and PPARγ in turn activates Nrf2 expression (39). Thus, ROSI would likely induce Nrf2 activity, whereas ROSI failed to decrease the high PA pressure in the hypoxic rats. Taking these findings into account, we surmise that the predominant contribution of Rho-kinase–mediated HPV could not be attenuated by Nrf2 activation or ROSI treatment. Therefore, PH could remain, although hypoxia-induced pulmonary vascular remodeling was efficiently decreased by oltipraz treatment or Keap1 knockdown.

Another potent Nrf2 activator, CDDO-imidazolide, has been shown to attenuate right heart dysfunction in a murine model of cigarette smoke–induced emphysema (40). Nrf2 activity protected against left cardiac hypertrophy, myocardial fibrosis and apoptosis, heart failure, and increased mortality in a murine heart failure model established by transverse aortic constriction (41). These findings suggested that Nrf2 might exert a direct cytoprotective function in cardiomyocytes under mechanical stresses such as excessive afterload. In the present study, our data also indicate a possible direct effect of Nrf2 on the RV, but we did not control for differences in RV afterload, which were likely present in $Nrf2^{-/-}$ mice. Isolated cardiac physiology experiments in a Langendorf model (42) would be helpful to answer these questions directly.

Hypoxic exposure has been shown to cause increased oxidative stress in whole lung tissue *in vivo* (7, 8) and in cultured bovine pulmonary endothelial cells *in vitro* (43). In this study, we directly confirmed ROS accumulation in the $CD31^{+}$ PVECs of hypoxia-exposed $Nrf2^{+/+}$ and $Nrf2^{-/-}$ mice by flow cytometry analyses using DCFDA. Expectedly, 2 days of hypoxia increased DCFDA levels in $CD31^{+}$ cells in $Nrf2^{+/+}$ and $Nrf2^{-/-}$ lung tissues. To further delve into these observations, we examined the mRNA expression levels of Nrf2 and Nrf2 downstream antioxidant genes in a $CD31^{+}$ cell fraction from the lungs of hypoxic $Nrf2^{+/+}$ and $Nrf2^{-/-}$ mice. Unexpectedly, Nrf2 and its target genes were differentially expressed in $CD31^{+}$ cells on exposure to hypoxia. GCLC and HO-1 mRNA expression in $Nrf2^{+/+}$ mice was down-regulated by hypoxic exposure despite ROS accumulation. There is accumulating evidence that the lungs of patients with respiratory disease and hypoxemia show increased oxidative stress. However, alveolar macrophages in patients with pulmonary emphysema exhibit decreased expression of the Nrf2 target genes (44). Although the mechanism underlying this observation is unknown, the down-regulation of antioxidants in those patients likely contributes to the disease progression. Therefore, forced induction of the antioxidant gene upon pharmacological induction of Nrf2 would elicit therapeutic efficacy to hypoxemic lung disease.

After exposure to hypoxia for 2 days, the NQO1 and GCLC immunoreactivity became barely detectable in the PA wall of WT mice. These data were consistent with the decreased expression of GCLC mRNA in the $CD31^{+}$ cells from hypoxia-exposed WT mice. However, the hypoxia-induced decrease in NQO1 expression in the whole lung was inconsistent with the constant NQO1 expression in the $CD31^{+}$ endothelial fraction. This observation might be explained by the differential distribution of GCLC and NQO1 in PA; NQO1 was mainly expressed in the PA

media, whereas GCLC expression was preferentially observed in the endothelium. Reduced NQO1 expression in the whole lung sample might be attributed to reduction of NQO1 in the PA media. Further analyses are necessary to evaluate antioxidant response in PA media under chronic hypoxia.

Another potential answer for the discrepancy may lie in the differences in the time-dependent changes of each Nrf2 target gene expression after hypoxia exposure. Several studies have demonstrated that the expression of the set of Nrf2 target genes was not always changed synchronously at the same time point after a single stimulus. For example, in the murine model of bleomycin-induced pulmonary fibrosis, the lung expression of GCLC mRNA, but not NQO1 and HO-1 mRNA, was significantly increased at 3 days after bleomycin injection (21). Meanwhile, the expression levels of NQO1 and HO-1 mRNA significantly increased at 7 days after bleomycin injection, whereas GCLC expression tended to decline at this time point. Another study using a neonatal murine model of hyperoxic lung injury demonstrated that the expression of several Nrf2 target genes in lung tissue was differentially altered for 3 days after the initiation of 100% O_2 exposure (45).

Our experimental design did not address the reason why some Nrf2 target genes were down-regulated despite an increase in ROS accumulation under hypoxic conditions. However, we surmised that hypoxia-inducible factor (HIF)1α could suppress the Nrf2 activity in the hypoxia-exposed lung. Mechanistic insight into functional crosstalk between Nrf2 and HIF1α systems has been largely obscured. It was reported that Nrf2-directed IL-8 and HO-1 expression was decreased by induction of HIF1α activity (46). Another group also demonstrated that tertiary butylhydroquinone–induced HO-1 expression was decreased by hypoxia (47). They suggested that the increased HIF1α–MafG interaction under hypoxia might deprive the dimerization partner from Nrf2, thereby suppressing Nrf2 activity. Further functional validation is needed to detail the exact mechanism.

TN-C exerts antiapoptotic and growth-stimulatory effect on vascular smooth muscle cells and is up-regulated in lung tissues of pulmonary hypertensive animals (19, 20, 48). In a rat model of monocrotaline-induced PH, TN-C expression in the pulmonary vasculature is up-regulated by oxidative stress (48). In bleomycin-induced lung fibrosis, TN-C is more abundantly accumulated in *Nrf2*$^{-/-}$ mice than in *Nrf2*$^{+/+}$ mice (21). Thus, Nrf2 activity presumably plays an important role in preventing aberrant TN-C accumulation in diseased lung. TN-C mRNA abundance was significantly increased after 1 week of hypoxia exposure, whereas the TN-C mRNA level was significantly decreased by oltipraz treatment. Immunohistochemical analyses with TN-C antibody demonstrated that the increased TN-C signal was localized in the external elastic lamina of the PA walls, especially at the level of the TB in hypoxic mice. Moreover, *Keap1*$^{f/f}$ mice showed significantly less TN-C signals in PA walls compared with hypoxic *Nrf2*$^{+/+}$ mice (Figures E4G, E4I, E4J, and E4L). The level of TN-C signals in the PA walls of hypoxic *Nrf2*$^{-/-}$ mice was comparable with that of nontreated hypoxic *Nrf2*$^{+/+}$ mice (Figures E4G, E4H, E4J, E4K). Comparable TN-C staining in lung tissues of hypoxia-exposed *Nrf2*$^{+/+}$ and *Nrf2*$^{-/-}$ mice may account for the similar extent of hypoxia-induced pulmonary vascular remodeling in these mice. Decreased TN-C immunoreactivity in the PA walls of oltipraz-treated hypoxic *Nrf2*$^{+/+}$ mice and hypoxia-exposed *Keap1*$^{f/f}$ mice suggested that oltipraz or *Keap1* knockdown decreases hypoxia-induced pulmonary vascular remodeling in part through inhibition of lung TN-C accumulation.

In our patient with COPD associated with PH, the expression of GCLC and NQO1 was diminished in the endothelial layers of PA walls, in good agreement with the decreased GCLC expression in CD31^{+} PVECs in hypoxia-exposed WT mice. However, IPAH lung showed strong GCLC and NQO1 signals in plexiform lesions and endothelial layers of thickened PA, presumably responding to oxidative stress (27). The differential response to ROS accumulation between COPD+PH and IPAH would provide attractive subjects for future studies, which would require another model of IPAH.

The present study showed for the first time that pharmacological and genetic activation of Nrf2 was capable of decreasing hypoxia-induced RVH and pulmonary vascular remodeling in a PH animal model. Nrf2 activators may prove to be a useful adjunct to currently available therapies for PH associated with respiratory diseases presenting with hypoxemia, such as COPD and IPF.

Author disclosures are available with the text of this article at www.atsjournals.org.

Acknowledgments: The authors thank Dr. Yoshihiro Fukumoto, Department of Cardiovascular Medicine, Tohoku University Graduate School of Medicine; Dr. Tsutomu Tamada, Department of Respiratory Medicine, Tohoku University Graduate School of Medicine; Dr. Shozaburo Doi, Department of Pediatrics and Developmental Biology, Tokyo Medical and Dental University; and Dr. Masayuki Noda, Department of Thoracic Surgery, Institute of Development, Aging and Cancer, Tohoku University for helpful discussions and Masako Honda, Department of Thoracic Surgery, Institute of Development, Aging and Cancer, Tohoku University for technical assistance.

References

1. Hultgren HN, Grover RF. Circulatory adaptation to high altitude. *Annu Rev Med* 1968;19:119–152.
2. Rabinovitch M, Gamble W, Nadas AS, Miettinen OS, Reid L. Rat pulmonary circulation after chronic hypoxia: hemodynamic and structural features. *Am J Physiol* 1979;236:H818–H827.
3. Stanbrook HS, Morris KG, McMurtry IF. Prevention and reversal of hypoxic pulmonary hypertension by calcium antagonists. *Am Rev Respir Dis* 1984;130:81–85.
4. Voelkel NF, Morris KG, McMurtry IF, Reeves JT. Calcium augments hypoxic vasoconstriction in lungs from high-altitude rats. *J Appl Physiol* 1980;49:450–455.
5. Lettieri CJ, Nathan SD, Barnett SD, Ahmad S, Shorr AF. Prevalence and outcomes of pulmonary arterial hypertension in advanced idiopathic pulmonary fibrosis. *Chest* 2006;129:746–752.
6. Minai OA, Chaouat A, Adnot S. Pulmonary hypertension in COPD: epidemiology, significance, and management: pulmonary vascular disease: the global perspective. *Chest* 2010;137:39S–51S.
7. Hoshikawa Y, Ono S, Suzuki S, Tanita T, Chida M, Song C, Noda M, Tabata T, Voelkel NF, Fujimura S. Generation of oxidative stress contributes to the development of pulmonary hypertension induced by hypoxia. *J Appl Physiol* 2001;90:1299–1306.
8. Matsui H, Shimosawa T, Itakura K, Guanqun X, Ando K, Fujita T. Adrenomedullin can protect against pulmonary vascular remodeling induced by hypoxia. *Circulation* 2004;109:2246–2251.
9. Lan AP, Xiao LC, Yang ZL, Yang CT, Wang XY, Chen PX, Gu MF, Feng JQ. Interaction between ROS and p38MAPK contributes to chemical hypoxia-induced injuries in PC12 cells. *Mol Med Rep* 2012;5:250–255.
10. Lewis MS, Whatley RE, Cain P, McIntyre TM, Prescott SM, Zimmerman GA. Hydrogen peroxide stimulates the synthesis of platelet-activating factor by endothelium and induces endothelial cell-dependent neutrophil adhesion. *J Clin Invest* 1988;82:2045–2055.
11. Liu LZ, Hu XW, Xia C, He J, Zhou Q, Shi X, Fang J, Jiang BH. Reactive oxygen species regulate epidermal growth factor-induced vascular endothelial growth factor and hypoxia-inducible factor-1alpha expression through activation of AKT and P70S6K1 in human ovarian cancer cells. *Free Radic Biol Med* 2006;41:1521–1533.
12. Ono S, Voelkel NF. PAF antagonists inhibit monocrotaline-induced lung injury and pulmonary hypertension. *J Appl Physiol* 1991;71:2483–2492.
13. Tuder RM, Chacon M, Alger L, Wang J, Taraseviciene-Stewart L, Kasahara Y, Cool CD, Bishop AE, Geraci M, Semenza GL, *et al*. Expression of angiogenesis-related molecules in plexiform lesions in severe pulmonary hypertension: evidence for a process of disordered angiogenesis. *J Pathol* 2001;195:367–374.

14. Weerackody RP, Welsh DJ, Wadsworth RM, Peacock AJ. Inhibition of p38 MAPK reverses hypoxia-induced pulmonary artery endothelial dysfunction. *Am J Physiol Heart Circ Physiol* 2009;296:H1312–H1320.
15. Itoh K, Mimura J, Yamamoto M. Discovery of the negative regulator of Nrf2, Keap1: a historical overview. *Antioxid Redox Signal* 2010;13: 1665–1678.
16. Itoh K, Wakabayashi N, Katoh Y, Ishii T, O'Connor T, Yamamoto M. Keap1 regulates both cytoplasmic-nuclear shuttling and degradation of Nrf2 in response to electrophiles. *Genes Cells* 2003;8:379–391.
17. Kobayashi A, Kang MI, Okawa H, Ohtsuji M, Zenke Y, Chiba T, Igarashi K, Yamamoto M. Oxidative stress sensor keap1 functions as an adaptor for Cul3-based E3 ligase to regulate proteasomal degradation of Nrf2. *Mol Cell Biol* 2004;24:7130–7139.
18. Taguchi K, Maher JM, Suzuki T, Kawatani Y, Motohashi H, Yamamoto M. Genetic analysis of cytoprotective functions supported by graded expression of Keap1. *Mol Cell Biol* 2010;30:3016–3026.
19. Cowan KN, Jones PL, Rabinovitch M. Elastase and matrix metalloproteinase inhibitors induce regression, and tenascin-c antisense prevents progression, of vascular disease. *J Clin Invest* 2000;105:21–34.
20. Hoshikawa Y, Nana-Sinkam P, Moore MD, Sotto-Santiago S, Phang T, Keith RL, Morris KG, Kondo T, Tuder RM, Voelkel NF, *et al*. Hypoxia induces different genes in the lungs of rats compared with mice. *Physiol Genomics* 2003;12:209–219.
21. Cho HY, Reddy SP, Yamamoto M, Kleeberger SR. The transcription factor Nrf2 protects against pulmonary fibrosis. *FASEB J* 2004;18:1258–1260.
22. Itoh K, Chiba T, Takahashi S, Ishii T, Igarashi K, Katoh Y, Oyake T, Hayashi N, Satoh K, Hatayama I, *et al*. An Nrf2/small Maf heterodimer mediates the induction of phase II detoxifying enzyme genes through antioxidant response elements. *Biochem Biophys Res Commun* 1997;236:313–322.
23. Hoshikawa Y, Voelkel NF, Gesell TL, Moore MD, Morris KG, Alger LA, Narumiya S, Geraci MW. Prostacyclin receptor-dependent modulation of pulmonary vascular remodeling. *Am J Respir Crit Care Med* 2001;164:314–318.
24. Fagan KA, Fouty BW, Tyler RC, Morris KG Jr, Hepler LK, Sato K, LeCras TD, Abman SH, Weinberger HD, Huang PL, *et al*. The pulmonary circulation of homozygous or heterozygous NOS-null mice is hyperresponsive to mild hypoxia. *J Clin Invest* 1999;103:291–299.
25. Sinha P, Clements VK, Ostrand-Rosenberg S. Reduction of myeloid-derived suppressor cells and induction of M1 macrophages facilitate the rejection of established metastatic disease. *J Immunol* 2005;174:636–645.
26. Eba S, Hoshikawa Y, Mitsuishi Y, Sato H, Watanabe T, Watanabe Y, Maeda S, Okada Y, Kondo T. An Nrf2 activator, oltipraz attenuates chronic hypoxia-induced cardiopulmonary alterations in mice [Abstract]. *Am J Respir Crit Care Med* 2011;183:A5487.
27. Bowers R, Cool C, Murphy RC, Tuder RM, Hopken MW, Flores SC, Voelkel NF. Oxidative stress in severe pulmonary hypertension. *Am J Respir Crit Care Med* 2004;169:764–769.
28. Benson AB III. Oltipraz: a laboratory and clinical review. *J Cell Biochem Suppl* 1993;17F:278–291.
29. Boone CW, Steele VE, Kelloff GJ. Screening for chemopreventive (anticarcinogenic) compounds in rodents. *Mutat Res* 1992;267:251–255.
30. Kensler TW, Egner PA, Dolan PM, Groopman JD, Roebuck BD. Mechanism of protection against aflatoxin tumorigenicity in rats fed 5-(2-pyrazinyl)-4-methyl-1,2-dithiol-3-thione (oltipraz) and related 1,2-dithiol-3-thiones and 1,2-dithiol-3-ones. *Cancer Res* 1987;47:4271–4277.
31. Moon RC, Kelloff GJ, Detrisac CJ, Steele VE, Thomas CF, Sigman CC. Chemoprevention of oh-bbn-induced bladder cancer in mice by oltipraz, alone and in combination with HPR and DFMO. *Anticancer Res* 1994;14:5–11.
32. Ramos-Gomez M, Kwak MK, Dolan PM, Itoh K, Yamamoto M, Talalay P, Kensler TW. Sensitivity to carcinogenesis is increased and chemoprotective efficacy of enzyme inducers is lost in nrf2 transcription factor-deficient mice. *Proc Natl Acad Sci USA* 2001;98:3410–3415.
33. Zhang Y, Munday R. Dithiolethiones for cancer chemoprevention: where do we stand? *Mol Cancer Ther* 2008;7:3470–3479.
34. Merrell MD, Jackson JP, Augustine LM, Fisher CD, Slitt AL, Maher JM, Huang W, Moore DD, Zhang Y, Klaassen CD, *et al*. The Nrf2 activator oltipraz also activates the constitutive androstane receptor. *Drug Metab Dispos* 2008;36:1716–1721.
35. Yu Z, Shao W, Chiang Y, Foltz W, Zhang Z, Ling W, Fantus IG, Jin T. Oltipraz upregulates the nuclear factor (erythroid-derived 2)-like 2 [corrected](NRF2) antioxidant system and prevents insulin resistance and obesity induced by a high-fat diet in C57BL/6J mice. *Diabetologia* 2011;54:922–934.
36. Rogers TK, Thompson JS, Morice AH. Inhibition of hypoxic pulmonary vasoconstriction in isolated rat resistance arteries by atrial natriuretic peptide. *Eur Respir J* 1997;10:2061–2065.
37. Crossno JT Jr, Garat CV, Reusch JE, Morris KG, Dempsey EC, McMurtry IF, Stenmark KR, Klemm DJ. Rosiglitazone attenuates hypoxia-induced pulmonary arterial remodeling. *Am J Physiol Lung Cell Mol Physiol* 2007;292:L885–L897.
38. Cho HY, Gladwell W, Wang X, Chorley B, Bell D, Reddy SP, Kleeberger SR. Nrf2-regulated PPARγ expression is critical to protection against acute lung injury in mice. *Am J Respir Crit Care Med* 2010;182:170–182.
39. Collins AR, Lyon CJ, Xia X, Liu JZ, Tangirala RK, Yin F, Boyadjian R, Bikineyeva A, Praticò D, Harrison DG, *et al*. Age-accelerated atherosclerosis correlates with failure to upregulate antioxidant genes. *Circ Res* 2009;104:e42–e54.
40. Sussan TE, Rangasamy T, Blake DJ, Malhotra D, El-Haddad H, Bedja D, Yates MS, Kombairaju P, Yamamoto M, Liby KT, *et al*. Targeting Nrf2 with the triterpenoid CDDO-imidazolide attenuates cigarette smoke-induced emphysema and cardiac dysfunction in mice. *Proc Natl Acad Sci USA* 2009;106:250–255.
41. Li J, Ichikawa T, Villacorta L, Janicki JS, Brower GL, Yamamoto M, Cui T. Nrf2 protects against maladaptive cardiac responses to hemodynamic stress. *Arterioscler Thromb Vasc Biol* 2009;29:1843–1850.
42. Bell RM, Mocanu MM, Yellon DM. Retrograde heart perfusion: the Langendorff technique of isolated heart perfusion. *J Mol Cell Cardiol* 2011;50:940–950.
43. Block ER, Patel JM, Edwards D. Mechanism of hypoxic injury to pulmonary artery endothelial cell plasma membranes. *Am J Physiol* 1989;257:C223–C231.
44. Goven D, Boutten A, Leçon-Malas V, Marchal-Sommé J, Amara N, Crestani B, Fournier M, Lesèche G, Soler P, Boczkowski J, *et al*. Altered Nrf2/Keap1-Bach1 equilibrium in pulmonary emphysema. *Thorax* 2008;63:916–924.
45. Cho HY, van Houten B, Wang X, Miller-Degraff L, Fostel J, Gladwell W, Perrow L, Panduri V, Kobzik L, Yamamoto M, *et al*. Targeted deletion of nrf2 impairs lung development and oxidant injury in neonatal mice. *Antioxid Redox Signal* 2012;17:1066–1082.
46. Loboda A, Stachurska A, Florczyk U, Rudnicka D, Jazwa A, Wegrzyn J, Kozakowska M, Stalinska K, Poellinger L, Levonen AL, *et al*. HIF-1 induction attenuates Nrf2-dependent IL-8 expression in human endothelial cells. *Antioxid Redox Signal* 2009;11:1501–1517.
47. Ueda K, Xu J, Morimoto H, Kawabe A, Imaoka S. MafG controls the hypoxic response of cells by accumulating HIF-1alpha in the nuclei. *FEBS Lett* 2008;582:2357–2364.
48. Aziz SM, Toborek M, Hennig B, Mattson MP, Guo H, Lipke DW. Oxidative stress mediates monocrotaline-induced alterations in tenascin expression in pulmonary artery endothelial cells. *Int J Biochem Cell Biol* 1997;29:775–787.